

Alma Mater Studiorum Università di Bologna
Archivio istituzionale della ricerca

Thermal integration of a SOFC power generator and a Na-NiCl₂ battery for CHP domestic application

This is the final peer-reviewed author's accepted manuscript (postprint) of the following publication:

Published Version:

Antonucci, V., Branchini, L., Brunaccini, G., De Pascale, A., Ferraro, M., Melino, F., et al. (2017). Thermal integration of a SOFC power generator and a Na-NiCl₂ battery for CHP domestic application. APPLIED ENERGY, 185, 1256-1267 [10.1016/j.apenergy.2016.04.051].

Availability:

This version is available at: <https://hdl.handle.net/11585/619885> since: 2020-02-10

Published:

DOI: <http://doi.org/10.1016/j.apenergy.2016.04.051>

Terms of use:

Some rights reserved. The terms and conditions for the reuse of this version of the manuscript are specified in the publishing policy. For all terms of use and more information see the publisher's website.

This item was downloaded from IRIS Università di Bologna (<https://cris.unibo.it/>).
When citing, please refer to the published version.

(Article begins on next page)

This is the final peer-reviewed accepted manuscript of:

Vincenzo Antonucci, Lisa Branchini, Giovanni Brunaccini, Andrea De Pascale, Marco Ferraro, Francesco Melino, Valentina Orlandini, Francesco Sergi,

Thermal Integration of a SOFC Power Generator and a Na-NiCl₂ Battery for CHP Domestic Application,

Applied Energy, Volume 185, 2017, p. 1256–1267

The final published version is available online at:

<http://dx.doi.org/10.1016/j.apenergy.2016.04.051>

©2017. This manuscript version is made available under the Creative Commons Attribution-NonCommercial-NoDerivs (CC BY-NC-ND) 4.0 International License (<http://creativecommons.org/licenses/by-nc-nd/4.0/>)

Thermal Integration of a SOFC Power Generator and a Na-NiCl₂ Battery for CHP Domestic Application

V. Antonucci¹, L. Branchini², G. Brunaccini¹, A. De Pascale^{2*}, M. Ferraro¹, F. Melino², V. Orlandini², F. Sergi¹

¹ CNR-ITAE, Salita S. Lucia sopra Contesse 5, Messina, 98126, Italy

²Università di Bologna, Viale del Risorgimento 2, 40136 Bologna, Italy

*corresponding author, e-mail: andrea.depascale@unibo.it, phone: +39-051-2093320

ABSTRACT

In this study the integration of a Solid Oxide Fuel Cell (SOFC) prime mover and a high temperature electrochemical Sodium Nickel Chloride (SNC) battery as storage has been investigated. The aim is to fulfil a domestic user energy demand and to reduce the primary energy consumption in comparison with a reference conventional scenario, thereby, to enhance the total efficiency in a μ -CHP (Combined Heat and Power) application on a yearly basis. A realistic operational sequence of the SOFC-battery integration has been calculated using simple logic conditions. Both thermal and electric integration have been considered, where the innovative thermal integration has been proposed in order to exploit the SOFC residual heat for the battery stand-by feeding. The key advantage of this system architecture is that the SOFC is operated without major load variations close to constant load, resulting in longer lifetime and thus reducing total costs of operation. The thermal integration provides additional advantages, as calculated in this study. Eventually, a comparison with alternative μ -CHP technologies has been carried out, highlighting the potential of the system based on the SOFC. Benefits are mainly shown in terms of primary energy savings and admissible costs.

Keywords: SOFC; micro CHP; Energy Storage; Sodium Nickel Chloride batteries.

NOMENCLATURE

Abbreviation

AUX	Auxiliary Boiler
CHP	Combined Heat and Power
EES	Electric Energy Storage
HX	Heat Exchanger
ICE	Internal Combustion Engine
MGT	Micro Gas Turbine
MRC	Micro Rankine Cycle
NET	External Electric Grid
SE	Stirling Engine
SNC	Sodium Nickel Chloride
SOFC	Solid Oxide Fuel Cell
TES	Thermal Energy Storage
TPV	Thermo-PhotoVoltaic
USER	Energy User

Symbols

C	Consumption [kWh]
E	Energy [kWh]
F	Cash Flow [€]
FP	Fuel input Power [kW]
i	index of year [-]
j	index of time step [-]
I	differential marginal cost [€]
N	number of years [-]
$NPES$	Net Primary Energy Saving [kWh/y]
NPV	Net Present Value [€]

52	<i>PEC</i>	Primary Energy Consumption [kWh/y]
53	<i>PED</i>	Primary Energy Demand [kWh/y]
54	<i>p</i>	electric efficiency reduction factor [-]
55	<i>P</i>	Power [kW]
56	<i>PD</i>	Power Demand [kW]
57	<i>r</i>	discount rate [-]
58	<i>RV</i>	Revenues [€]
59	Δt_i	time interval [s]
60	η	efficiency [-]

61
62 *Subscripts and Superscripts*

63	<i>el</i>	electric
64	<i>NG</i>	Natural Gas
65	<i>pur</i>	purchased
66	<i>ref</i>	reference
67	<i>sb</i>	stand-by
68	<i>sold</i>	sold
69	<i>th</i>	thermal
70		

71 1. INTRODUCTION

72 Domestic applications of innovative small scale Combined Heat and Power (CHP) prime movers are currently under
73 attention (an overview of technologies is provided in [1]), in order to locally fulfil the internal energy demand, reducing
74 access to the external net and limiting primary energy consumption (see the review by Angrisani et al. [2]). Different recent
75 studies are focused on CHP modelling and optimization in the framework of domestic and district heating applications [3-5],
76 where it is feasible to replace or integrate current heating systems, thus achieving energy savings. Micro-CHP generation
77 implemented nearby the domestic energy user can affect also the environmental performance, with local and global effects
78 and possible improvements in terms of greenhouse gas, nitric oxide and carbon oxide emission reduction, under properly
79 selected boundary conditions (as shown for many prime movers in a previous study of the authors [6]).

80 Among CHP technologies, high temperature fuel cells offer high electric performance, e.g. Solid Oxide Fuel Cell (SOFC)
81 expected electric efficiency is about 50-60% [7], values comparable with current large power station efficiency, as reviewed
82 in [8]. Advantages are related to the fact that fuel cells systems allow to avoid thermodynamic efficiency limitations due to
83 combustion, occurring in other more conventional micro generators (such as reciprocating engines and microturbines) or in
84 other small size heat recovery power technologies (such as micro-Rankine cycles and Stirling engines). The CHP application
85 for residential building of a PEM technology fuel cell has been investigated in [9], where possible layouts and thermal
86 integrations with the user are shown. Moreover, SOFC could provide significant amount of high value heat, in comparison
87 with other fuel cells (see for example [10,11]), leading to potential values of overall CHP efficiency as high as 80-85% [12].

88 The penetration of fuel cell systems as CHP prime mover in the residential sector is expected to grow, especially if supporting
89 schemes and policies will be applied in the near future [13]. The SOFC technology applicability has been demonstrated in
90 modelling studies for commercial buildings [14]. Nevertheless, transient capability of SOFC is quite limited, requiring
91 additional design efforts and subsystems [15] to cope with variable load demand.

92 An effective strategy to improve SOFC utilization in micro-grid applications is to apply electric and/or thermal load shift, as
93 shown for example in [16]. Local storage can be also applied for peak shaving both in case of non-programmable renewable
94 and μ -CHP generators, where proper energy management logic should be functional in order to ensure power supply to user
95 [17]. In particular SOFC utilization factor can be improved via energy storage devices, to cope with the instantaneous
96 demand-production mismatch, typically occurring in residential buildings.

97 Several storage technologies are available, with the electrochemical devices best suited for small capacity and modular
98 installations, due to the technology readiness, with limited size, cost and high flexibility compared to kinetic, hydraulic,
99 compressed-air, or super-capacitor storage solutions [18].

100 Sodium/Nickel Chloride (SNC) electrochemical storage devices, also known in the past as ZEBRA batteries, are intrinsically
101 maintenance free, show long life and high reliability with limited self-discharge and are fully recyclable [19]; specific energy
102 of the SNC battery is able to achieve values in the range 90–120 Wh/kg, energy density can be up to 150 Wh/l, and specific
103 power is in the range 150–170 W/kg [20]; large-scale stationary storage application has been demonstrated [21]. Moreover,
104 SNC are operated at high temperature, typically around 270°C [22]; thus, SNC could be an option for SOFC integration and
105 thus they have been taken into account here.

106 A complementary study on SOFC and SNC integration for vehicular application had been performed by Aguiar et al. in [23],
107 showing the potential benefits of extended range and more rapid response of the hybrid system to variable loads.

108 The aim of the study carried out and described in this paper is to investigate performance of a thermally integrated SOFC-SNC
109 battery system network, in order to assess if the battery could improve the CHP operation of the SOFC in a domestic
110 application long term scenario. A preliminary study on the SOFC-SNC system was previously performed in [24], where,
111 nevertheless, the full thermal integration, investigated here, was not considered. In particular, the new content of this paper
112 is the analysis of the SOFC-SNC performance when a part of the heat released for the SOFC is directly used to heat the SNC in
113 stand-by periods, reducing in this way the external energy supply to the system, currently realized in actual SNC models by
114 means of electric resistance (as instead considered in [24]). The authors are not aware of previous investigations of this kind
115 of new arrangement. In order to perform this study, some experimental data acquired on a SOFC generator have been
116 presented and used to determine the actual available heat characteristics. These data are in line with other recent
117 experimental studies on SOFC [25]; nevertheless, such data have not been used before as in this paper, for assessing a
118 possible thermal integration of SOFC with SNC batteries, not included in the previous study [24].

119 2. SOFC CHARACTERISTICS AND EXPERIMENTAL PERFORMANCE

120 In this study, a small scale pre-commercial Intermediate Temperature SOFC system, manufactured by SOFCpowerTM, rated
121 for 500 W of electric power output, has been taken into account as reference μ -CHP device. Nameplate data of the SOFC
122 system are reported in Table 1 and the internal SOFC layout (comprising a 36 cell stack, a fuel pre-reformer, an after-burner
123 and a cathode air pre-heater [26]) is provided in Fig. 1; the internal temperature levels, registered during measurements
124 performed with the SOFC run at base load, are also highlighted in figure. More details on the experimental facility and the
125 carried out tests boundary conditions are also provided in [26]. Some experimental performance data of the SOFC generator,
126 acquired for this study, are collected in Figs 2 to 4.

127 In particular, Fig. 2a shows the stack current, voltage and power values measured during a 200 hours test carried out at the
128 CNR laboratories. During the performed tests, the stack reached a stable load and voltage-current condition, with base load
129 data as summarized in Table 2, leading to instantaneous electric efficiency values close to 40%, and with a minimum heating
130 up process time equal to 220 min. As shown in Fig. 2a, in a cold start-up sequence, after an early purging interval, the tested
131 SOFC system needs approximately 3-5 hours to reach stable base load conditions, by applying a heating ramp rate in the
132 range 2-5°C/min, prescribed by the manufacturer, in order to avoid mechanical stress in the internal stack components.
133 During the experiment, temperature values in different locations of the stack (top, base and average) have been monitored;
134 the recorded values, reported in Fig.2b for a time window covering the stable base-load time conditions, show stack
135 temperature local values, ranging between 730 and 750 °C, with limited excursions. Moreover, Fig. 3a shows the recorded
136 (quite constant) temperature profiles of the ambient air, of the cathode inlet air and of the exhaust gas temperature (after
137 the afterburner) during the performed base load test.

138 Figure 3b instead refers to part load conditions and it presents the SOFC performances, in terms of exhaust gas temperature
139 and mass flow rate; by reducing the SOFC load, the exhaust gas temperature dropped from 570°C (at full load) down to
140 450 °C (at 20 % of full load), while exhaust gas flow remained almost constant, with a very slight increase.

141 Eventually, the fuel cell polarization curve and the power curve are shown in Fig. 4a, while Fig. 4b reports the calculated full-
142 load and part-load performance in terms of electric and thermal efficiency, with reference to the inlet fuel Lower Heating
143 Value: in particular, the thermal efficiency was obtained by cooling the SOFC system exhaust gas down to 300°C, by using an
144 external heat exchanger with water as cold fluid. In the following simulations, the SOFC generator has been supposed
145 working at full load or it is switched off, avoiding part load conditions, thus without affecting the system performance. This is
146 common behavior in residential applications (see Barbieri et al. [27], Dentice d'Accadia et al. [28]) and other CHP cases (e.g.,
147 [29]), compared to electric load following. Moreover, given the long time required by the SOFC to turn on in "cold" start-up
148 conditions, only "hot" start-up has been taken into account. The heat for the SOFC start-up sequence can be supplied by
149 additional fuel and using an auxiliary burner (in Fig. 1 [26]) or an electric heater [30], which allows to preheat the "hot box",
150 where the stack is physically confined. If the SOFC system is kept in hot stand-by conditions for short times, the SOFC remains
151 close to operating temperature conditions, with reduced energy consumption in comparison with the cold start-up.

152 3. SNC BATTERIES CHARACTERISTICS

153 The above introduced SOFC system has been integrated with an electrochemical storage device. The considered battery is
154 based on the Sodium-Nickel Chloride (SNC) technology, where the positive electrode is made of NiCl_2 and the negative
155 electrode is liquid state Sodium, as far as the operating temperature is above 157°C [19]. Nevertheless, the optimal operating
156 temperature of the SNC battery is in the range 270-300 °C (thus, SNC belong to the high temperature battery typology),
157 which is compatible with the SOFC outlet temperature. In particular, the considered battery is a commercial Fiamm 48TL80
158 model, developed for stationary applications and rated for almost 4 kWh of nominal capacity with energy density equal to 81
159 Wh/kg and 80 Wh/liter, as reported in Table 3, providing the SNC main characteristics. In a previous study of the authors [24]
160 where different battery size were considered, the selected SNC module capacity was found beneficial when electrically
161 integrated with the SOFC in study (resulting in a storage capacity-to-generator power size ratio equal to 4kWh/0.5kW);

indeed, this size, in comparison with larger capacities, was shown able to minimize energy purchased from the external net and to achieve higher values of savings in primary energy, for the same domestic application.

The optimal charging load curves of the SNC battery are presented in Fig. 5 [19, 20]: the power input should be limited (to 1.2 kW) and the ideal charging time is equal to 5 h. More in details, the charging load curves in Fig. 5a show two phases: the first part of the charging curve, with a duration of approximately 2.5 hours, allows to reach 70% of the full State of Charge (SOC) and it is characterized by quite constant voltage and current (see Fig. 5b). During the second part, the SNC reaches the full SOC with a decreasing trend vs time of both current and power.

Due to the SNC ceramic electrolyte operating temperature requirements (which should constantly remain above 200-250°C), an energy absorption should be taken into account during stand-by periods of the battery, in order to keep high and constant the SNC internal temperature. The power required by the SNC battery stand-by, has been roughly estimated equal to 110 W, according to available data by manufacturer. This stand-by power is commonly provided by an electric resistance, in commercial SNC modules; this SNC conventional operating condition has been named here as “electric stand-by” absorption case. In this study, an innovative configuration, named as “thermal stand-by”, has been also investigated; in this new SNC configuration, the stand-by power is considered directly provided by the SOFC as thermal power; this can be obtained by recovering waste heat available into the SOFC exhaust gas flow. An energy comparison between the conventional and innovative configuration is carried out in this study and an appropriate CHP performance calculation for the integrated system involving the SNC storage is developed.

4. INTEGRATED SOFC-SNC SYSTEM NETWORK FOR DOMESTIC APPLICATION

A CHP system network based on the SOFC and the SNC battery is under investigation in this study for stationary domestic application. The considered network layout, with the included subcomponents, is shown in Fig. 6. The main included components are: (i) the SOFC based power generator, (ii) the SNC battery, indicated here also as Electric Energy Storage (EES) system; (iii) the external electric net (NET); (iv) a Thermal Energy Storage (TES) system; (v) an auxiliary boiler (AUX); (vi) a power absorber or user (USER).

The network related power flows exchanged between components are also shown in Fig. 6, where the electric power flows are in blue and the thermal ones in red. In particular, due to the CHP arrangement, the USER is characterized by both a thermal and an electric power load (indicated as PD_{el} and PD_{th} respectively, in Fig. 6). The SOFC system, working as a μ -CHP generator, produces both electric and thermal power ($P_{el,CHP}$ and $P_{th,CHP}$ respectively). The USER electric power demand can be satisfied by the SOFC production, by the EES ($P_{el,EES}$) or by the NET ($P_{el,NET}$); the EES and NET power flow terms can be also negative, in case of power absorption by each of the two subsystems.

The user thermal demand PD_{th} can be fulfilled by the thermal power production of the SOFC ($P_{th,CHP}$), by the TES thermal output ($P_{th,TES}$) or, if necessary, by the auxiliary boiler production ($P_{th,AUX}$), with a consequent additional fuel consumption.

The TES system is able to provide thermal power (positive flow term) or to store it (negative), as shown in the figure. The optimal size of the TES has been evaluated in a previous work [28], where a correlation between the TES capacity, the CHP thermal size, the thermal demand and the operational hours of the CHP prime mover was estimated: over a certain TES capacity, the total amount of operational hours does not increase. The optimal volume size of the TES coupled with the SOFC generator selected in this study has been considered equal to 500 liters.

In order to fulfill the SNC stand-by thermal demand, two possible network configurations have been taken into account and compared in this study, named respectively *thermal stand-by* and *electric stand-by*. The first configuration is proposed here as a new solution not yet implemented in SNC batteries, while the second one is a conventional arrangement. In the first case of *thermal stand-by*, the stand-by thermal power is considered directly supplied by the SOFC ($P_{th,SB}$, indicated by the red dotted line in Fig. 6), by recovering the waste heat available into the SOFC exhaust gas flow. In the other *electric stand-by* case, the thermal power is provided by an electric resistance, fed by the SOFC system through the NET ($P_{el,SB}$, shown by the dotted blue line in Fig. 6). This case was preliminary investigated in [24] and it corresponds to the normal SNC management. In the *thermal stand-by* case instead, the SNC electric consumption for stand-by is eliminated ($P_{el,SB} = 0$) and the $P_{th,SB}$ is considered in the calculations as an additional contribution available for the thermal demand. It should be finally mentioned that apart from SNC stand-by periods, during operation in charging and discharging mode, the SNC battery produces additional heat, which is normally dissipated. For sake of simplicity this wasted heat has not been included in the system thermal balance, thus performing a more cautious CHP production estimation.

Integrated SOFC-SNC system network simulation

A reasonable management logic of the system components has been taken into account and a calculation routine has been developed in MS Excel and Visual Basic language, to calculate the electric and thermal power flows for each j^{th} time-step (hour or minute basis) of the considered year, as described below. Fig. 7a shows the conventional calculation routine developed, taking into account the basic *electric stand-by* mode, while Fig. 7b presents the calculation routine elaborated to analyze the energy flows exchange, in the innovative *thermal stand-by* configuration. A thermal flows subroutine and an electric flows subroutine are included in the developed numerical procedure, as visible in the figures. More in details, the

complete calculation routine requires various input data: (1) the design data of the CHP prime mover, i.e., nominal electric power, electric efficiency and the ratio between electric and thermal production; (2) the capacity of the EES and the TES; (3) the electric and thermal load required by the user (daily demand normalized to the peak value and seasonal fluctuation correction factor). The main output data of the calculation routines are: (1) the on/off sequence of the CHP generator; (2) the total operating hours; (3) the yearly thermal and electrical production; (4) the energy flow exchanged; (5) the resulting performance in terms of total saving of primary energy and costs.

A “thermal load following” μ -CHP operation mode is assumed, i.e. the thermal power load demand commands to switch on the SOFC, while the electric production has been considered as a surplus production, sent to the user if necessary, otherwise stored into the EES or sold to the external grid. Actually, in both cases of Fig. 7a and Fig. 7b, the electric flows occurrence depends on the results obtained from the thermal subroutine and therefore the electric calculation is performed once the thermal calculation is run. For each j^{th} period of time, the developed routines satisfy the following balance equations:

$$PD_{th}(j) = P_{th,CHP}(j) + P_{th,TES}(j) + P_{th,AUX}(j) \quad (1)$$

$$PD_{el}(j) = P_{el,CHP}(j) + P_{el,EES}(j) + P_{el,NET}(j) \quad (2)$$

The thermal power demand of the user is fulfilled by the SOFC thermal output, by the TES output and by the AUX output, with this order of priority, as the equation (1) reports. If a surplus of the μ -CHP thermal production occurs in comparison with the instantaneous PD_{th} , the surplus is stored in the TES and the AUX is switched-off. Fig. 8 presents in details the thermal flows subroutine introduced and it highlights the priorities and limitations. In particular:

- the SOFC and the AUX are switched off when the demand is lower than $P_{th,TES}$;
- the SOFC is switched on (at full load) when the demand is higher than the power due to residual TES storage capacity;
- if PD_{th} is larger than $P_{th,CHP}$, the load is satisfied by the available energy stored in the TES and by the auxiliary boiler. On the contrary, if PD_{th} is lower than $P_{th,CHP}$, the TES is filled as much as possible.
- it is not allowed to dissipate the thermal energy produced by SOFC. Therefore, if the TES is full, the SOFC is turned off and the load requested is satisfied by the TES with the help of the auxiliary boiler.

For what concerns the electric flows, the electric power demand (PD_{el}) is fulfilled by the SOFC electric output ($P_{el,CHP}$), by the EES output ($P_{el,EES}$) and by the NET contribution ($P_{el,NET}$), with the given order of priority (equation (2)). Fig. 9 shows the electric subroutine, with the electric priorities and the logic management introduced into the calculation code. More in details:

- if the SOFC is switched off (and consequently $P_{el,CHP}=0$), the load demanded is satisfied by the available energy stored in the EES. If it is not sufficient, the remaining part is purchased from the external grid;
- if $P_{el,CHP} > 0$ and it is higher than PD_{el} , the electric power surplus is stored in the EES. If the EES is in its maximum SOC condition, the surplus is delivered to the NET. Otherwise, if the electric demand is higher than the μ -CHP generation plus the EES power contribution, the NET provides the residual electricity;

As shown in Fig. 7a and Fig. 7b, in both cases, the SOC of the EES and the level of the TES are updated at each j^{th} time step. In particular, Fig. 7b shows the explicative scheme of the iterative routine, considering the innovative *thermal stand-by* configuration. The stand-by periods occurrence depends on the electric power flows, which are depending on the thermal flows, according to the used “thermal load following” management logic. Thus, in this case of *thermal stand-by*, an iterative calculation procedure has been implemented, in order to obtain the final electric and thermal flows, including the SNC stand-by thermal power flows.

In order to realize an optimal configuration, the hot gas line downstream the SOFC has been adapted and improved with the introduction of two heat exchangers, namely HX1 and HX2. As visible in Fig. 10, HX1 is located upstream the EES, to cool the exhaust gas to a temperature level compatible with the SNC battery optimal operation and HX2 is downstream the battery, to recover additional thermal power, available for the domestic user.

The operating SNC battery temperature has been set equal to 270°C, the exhaust gas temperature after HX1 equal to 350°C and after HX2 equal to 120°C. The cooling water outlet/return temperature constraints have been set equal to 60°C/90°C respectively, compatible with a conventional domestic user.

The yearly electric and thermal load profiles of a typical single domestic USER have been taken into account in this study, as elaborated in [15]. More in details, Fig. 11 reports the yearly monotonic curves and the daily profiles of thermal and electric USER demand, normalized versus the peak values, respectively equal to 12.6 kW and 2.3 kW. In the Fig. 12b the thermal demand is split in hot water and heating demand. These data are representative of a possible dwelling condition in temperate latitudes zone and they have been used as input in the developed calculation routine.

5. SUMMARY OF RESULTS AND COMPARISON WITH OTHER PRIME MOVERS

Table 4 provides a summary of the evaluated yearly electric and thermal energy flows. Given the above described load demand and the SOFC operation management assumptions, the calculated number of SOFC operating equivalent hours results equal to the entire thermal year (i.e., 4392 h), in both the *thermal stand-by* and *electric stand-by* scenarios. As a

result, the SOFC generator provides the same amount of electric energy in both scenarios, as shown in Table 4 (SOFC electric output), but a difference occurs in the amount of energy provided to the NET (From SOFC to NET), due to the EES stand-by periods electricity absorption in the *electric stand-by* scenario.

In both scenarios, the SOFC is able to cover the entire USER electricity demand (equal to 1458 kWh), with a useful overproduction (equal approximately to 47% of the yearly demand, in the *thermal stand-by* scenario, and to about 34% of the demand, in the *electric stand-by* scenario) delivered mainly to the NET. The electric consumption for the EES stand-by operation, in the *electric stand-by* scenario, is about 13% of the USER demand, less than 9% of the SOFC production and equal to 25% of the energy absorbed by the EES (for storage and stand-by purpose). The total energy stored in the EES, due to instantaneous surplus periods of production occurring along the year, is equal to about 38% of the total electricity demand.

On the contrary, in both scenarios, the SOFC thermal production is remarkably lower than the USER thermal energy demand, covering approximately only 12% of it, leading to a significant contribution delivered by the auxiliary boiler. The SNC thermal energy consumption in the stand-by scenario represents approximately only 1% of the USER thermal demand (it is less than 8% of the SOFC thermal production), requiring an equal, very limited, additional contribution from the AUX boiler.

Thus, the carried out comparison between the two scenarios shows the possibility to increase the amount of electricity sold to the NET, with a limited negative impact on the thermal energy provided by the AUX boiler, by implementing the *thermal stand-by* configuration.

Using the calculated power flows, a comparison between the two scenarios can be carried out in terms of the thermal and electric overall system efficiency, respectively calculated as:

$$\eta_{th_system} = \frac{\sum_j \Delta t_j \cdot PD_{th,j}}{\sum_j \Delta t_j \cdot FP_{SOFC,j} + \sum_j \Delta t_j \cdot FP_{AUX,j}} \quad (3)$$

$$\eta_{el_system} = \frac{\sum_j \Delta t_j \cdot PD_{el,j} + \sum_j \Delta t_j \cdot P_{el,NET,j}}{\sum_j \Delta t_j \cdot FP_{SOFC,j} + \sum_j \Delta t_j \cdot FP_{AUX,j}} \quad (4)$$

where Δt_j is the time duration of the j -th period in which each power flow is calculated (assumed constant and equal to 5 minutes); in particular, both the fuel input contributions at the SOFC ($FP_{SOFC,j}$) and at the auxiliary boiler ($FP_{AUX,j}$) are taken into account; the useful thermal and electric production entering the USER ($PD_{th,j}$ and $PD_{el,j}$) are considered as output and, in case of the electric system efficiency, also the net power flow toward the external electric network ($P_{el,NET}$) is included. Using definitions of eq. (3) and eq. (4) the thermal system efficiency is equal to 79.5% in the *thermal stand-by* scenario and equal to 80.2% in the *electric stand-by* scenario, while the electric system efficiency is equal to 8.5% in the *thermal stand-by* scenario and equal to 7.8% in the *electric stand-by* scenario. This gain in electric system efficiency is clearly due to the avoided electric consumption for the SNC battery stand-by periods. It should be highlighted that the η_{el_system} calculated according to eq. (4) takes into account all the fuel introduced into the integrated system (including the AUX fuel consumption) and thus it is not equal to the prime mover electric efficiency (see η_{el} values in Table 5).

Comparison with other prime movers

A further comparison has been performed between the fuel cell based prime mover in study and various alternative μ -CHP systems [27] in the range of power size up to 5 kW, based on different conventional and under development technologies, as provided in [24], namely three ICEs, two Stirling Engines (SE), two Micro Rankine Cycles (MRC), one Micro Gas Turbine (MGT), and a Thermo-PhotoVoltaic (TPV) generator prototype, described in [31]. Table 5 presents the main prime movers data used as input in the developed calculation routine, i.e., the electric power size, the nominal electric and thermal efficiency values, the ratio between electric and thermal production at full power (named C in the table) and the TES volume. The TES optimum size has been estimated, according to the study carried out in [32], for each considered prime mover. While the SOFC prime mover has the highest nameplate electric efficiency among the selected units, the Stirling engine, the MRC and TPV systems are characterized by higher thermal than electric performance.

The considered prime movers have been integrated with the selected SNC battery in study. Both SNC *stand-by* strategies have been taken into account and compared for the systems composed by the prime mover and the battery. The calculated number of operational hours and the SNC stand-by hours are reported in Fig. 12. Fig.12a shows that the SOFC prime mover leads to the highest value of operational hours, compared to the other solutions, due to the low electric power size, best fitted for the domestic USER in study, and also due to the highest electric efficiency. The 1 kW ICE#1 provides similar but

lower operating hours, while the other compared systems operate for remarkably lower number of hours per year. This result can be due to the fact that these CHP systems are characterized by a higher power size and a lower electric efficiency (i.e. higher residual thermal power), which leads to a higher capability to cover the thermal demand of the user. SNC stand-by hours is approximately equal to 1700 h for the SOFC system (see Fig. 12.b), it is much higher (around 3100 h) for the ICE#1 and lower than the SOFC case in all the other cases. Hence, it can be observed that systems which are operated for a higher number of operating hours along the year also tend to be characterized by a higher number of stand-by hours; indeed, due to the larger size, they are able to fulfill the demand producing also a larger amount of surplus power, stored and available for the user during stand-by periods. Not significant differences occur between the *thermal stand-by* and the *electric stand-by* scenario, in terms of both prime mover operation and stand-by hours; thus, this result shows that the *thermal stand-by* implementation does not significantly alter the CHP system operation, once the prime mover is defined.

Figure 13 shows the calculated thermal and electric system efficiency values for all the considered μ -CHP systems. In particular, the thermal system efficiency value for the SOFC case (around 80%) is in line with the highest values for the other systems (Fig. 13.a); SOFC and TPV based μ -CHP systems are characterized by the lowest power size and show lowest values of the overall electric system efficiency (respectively close to 8% and to 6%, in Fig. 13.b); the largest values of electric system efficiency are obtained with the prime movers with larger power size (ICE#2, ICE#3, SE#2 and MGT, showing values up to 26%), because they allow to cover a higher fraction of the user electric energy demand. These results can be also used as a first guidance in real applications, where the size and technology of the μ -CHP system must be selected for a similar demand size of users.

The integrated μ -CHP-EES systems under investigation using different prime movers have been also compared in terms of CHP performance on yearly basis. The analysis has been based on the yearly Net Primary Energy Saving (*NPES*), calculated as:

$$NPES = PED - PEC \quad (5)$$

where: *PED* (Primary Energy Demand) is the primary energy required to fulfil the CHP USER electric and thermal demand in a reference non-CHP scenario; *PEC* (Primary Energy Consumption) is the actual primary energy consumption due to the μ -CHP generator operation. Thus, *NPES* is a differential indicator, showing the savings achievable with the adoption of the CHP-EES integrated system, with respect to a reference situation, in which the required electric energy is acquired from the external net and the thermal energy demand is entirely covered by an auxiliary reference boiler. The *PEC* and *PED* terms can be calculated according to eq. (6) and eq. (7) respectively:

$$PEC = \frac{E_{el,CHP}}{\eta_{el,CHP}} + \frac{E_{el,pur} - E_{el,sold} - E_{el,EES}}{p \cdot \eta_{el,ref}} + \frac{E_{th,AUX}}{\eta_{th,ref}} \quad (6)$$

$$PED = \frac{PD_{el}}{p \cdot \eta_{el,ref}} + \frac{PD_{th}}{\eta_{th,ref}} \quad (7)$$

where $E_{el,CHP}$ represents the electric energy produced by the CHP prime mover in the considered period; $E_{el,pur}$ is the electric energy acquired by the net; $E_{el,sold}$ is the electric energy sold to the net; $E_{el,EES}$ is the electric energy stored at the end of the considered period in the EES; $E_{th,AUX}$ is the thermal energy produced by AUX; $\eta_{el,CHP}$ is the electric efficiency of the CHP generator. Moreover, $\eta_{el,ref}$ and $\eta_{th,ref}$ are the reference efficiency values for the electric and thermal energy separate production (assumed respectively equal to 0.522 and 0.90 in this study, in line with European regulation on CHP [33]) and p is a non-dimensional correction factor (assumed equal to 0.86 [33]), which takes into account the energy losses on the electric net.

Fig. 14a and 14b provide the *NPES* index value per installed electric power of the investigated μ -CHP prime mover, for *electric stand-by* and *thermal stand-by* respectively. The SOFC-based μ -CHP system provides values of savings in primary energy around 1500-1800 kWh/year, corresponding to 3500-4000 kWh per installed kW, values larger than in the other technologies (only case of SE#1 can reach slightly larger values). According to the obtained results, the μ -CHP generators with higher power size show lower values of normalized *NPES*. The *thermal stand-by* case provides better performance in comparison with the *electric stand-by*, with a gain of around 500 kWh/y/kW in case of SOFC.

Eventually, a simplified comparative economic analysis has been performed to ascertain the viability of the proposed integrated system with respect to the reference non-CHP scenario. In particular, the maximum admissible cost of the μ -CHP system which allows to obtain a breakeven point has been calculated. The values assumed in the economic analysis are reported in Table 6, considering data compatible with the Italian electricity and natural gas tariff scenario, but also in line or conservative with respect to the European context. The Net Present Value (*NPV*) has been set equal to zero, as in eq. (8), in order to determine the max admissible differential marginal cost (I) of the μ -CHP system:

$$NPV = -I + \sum_{i=1}^N \frac{F_i}{(1-r)^i} = 0 \quad (8)$$

where F_i represents the cash flow of the i^{th} year, calculated as:

$$F_i = RV_{E,el} - E_{el,pur} - (C_{NG})_{CHP} + (C_{NG})_{AUX} \quad (9)$$

where: $RV_{E,el}$ is the revenues for electric energy surplus; $E_{el,pur}$, the electric energy purchase from the net; $(C_{NG})_{CHP}$, the fuel consumption of the CHP generator; $(C_{NG})_{AUX}$, the avoided boiler fuel consumption.

Fig. 15 shows results of the admissible investment cost of the μ -CHP system per unit of installed electric power: larger values of admissible investment cost, in the range of 2500-3000 €/kW, occur in case of the SOFC-SNC integrated system and the values obtained are almost the same in the EES *thermal stand-by* and *electric stand-by* case.

According to Fig. 15, also the economic performance shows a decreasing trend versus the μ -CHP generators power size. This is due to the fact that the new proposed solution allows to save an amount of electricity not wasted in stand-by periods. Thus, finally, these economic results offer also a general guidance for selecting a proper sizing of the components or to understand if existing/future SNC battery technology modules can be competitive.

6. CONCLUSIONS

The carried out study, on a SOFC generator integrated with a SNC storage in order to obtain a μ -CHP system for domestic application, showed the viability of the system, in terms of overall energy and economic performance. The paper, based on experimental data acquired on a μ -SOFC stack and on commercially available SNC battery data, showed the possibility to thermally integrate the two components. The considered innovative system allows to achieve thermal and electric system efficiency values close to 80% and 7% respectively, including also the input fuel of the required auxiliary boiler. The calculated primary energy savings can achieve values around 4000 kWh/y/kW and the admissible costs, obtained with the simplified economic analysis under a selected reference economic scenario, can be estimated up to around 3000 €/kW. These values are promising, if compared with values calculated for other μ -CHP technologies, such as the conventional internal combustion engine, or other under development systems, e.g.: micro-Rankine cycles, micro-turbines, Stirling engines and thermo-photo-voltaic systems.

REFERENCE

- [1] V. Kuhn, J. Klemeš, I. Bulatov. MicroCHP. Overview of selected technologies, products and field test results. Applied Thermal Engineering 28 (2008) 2039-2048.
- [2] G. Angrisani, C. Roselli, M. Sasso. Distributed microtrigeneration systems. Progress in Energy and Combustion Science 38 (2012) 502-521.
- [3] S. Seijo, I. del Campo, J. Echanobe, J. García-Sedano. Modeling and multi-objective optimization of a complex CHP process. Applied Energy, Volume 161, 1 January 2016, pp. 309-319
- [4] H. Wang, W. Yin, E. Abdollahi, R. Lahdelma, W. Jiao. Modelling and optimization of CHP based district heating system with renewable energy production and energy storage. Applied Energy, Volume 159, 1 December 2015, pp. 401-421
- [5] T. C. Fubara, F. Cecelja, A. Yang. Modelling and selection of micro-CHP systems for domestic energy supply: The dimension of network-wide primary energy consumption. Applied Energy, Volume 114, February 2014, pp. 327-334
- [6] M. Bianchi, L. Branchini, A. De Pascale, A. Peretto. Application of Environmental Performance Assessment of CHP Systems with Local and Global Approaches. Applied Energy 130 (2014) 774-782.
- [7] S. Campanari. Thermodynamic model and parametric analysis of a tubular SOFC module. Journal of Power Sources 92 (2001) 26-34.
- [8] R. K. Bhargava, M. Bianchi, S. Campanari, A. De Pascale, G. Negri di Montenegro, A. Peretto. A Parametric Thermodynamic Evaluation Of High Performance Gas Turbine Based Power Cycles. Transaction of the ASME, Journal of Engineering for Gas Turbines and Power 132 (2010) 022001-1/14.
- [9] A. Adam, E. S. Fraga, D. J.L. Brett. Options for residential building services design using fuel cell based micro-CHP and the potential for heat integration. Applied Energy, Volume 138, 15 January 2015, pp. 685-694
- [10] B. Belvedere, M. Bianchi, A. Borghetti, A. De Pascale, M. Paolone, R. Vecchi. Experimental analysis of a PEM fuel cell performance at variable load with anodic exhaust management optimization. International Journal of Hydrogen Energy 38 (2013) 385-393.
- [11] M. Bagnoli, B. Belvedere, M. Bianchi, A. Borghetti, A. De Pascale, M. Paolone. A feasibility study of an auxiliary power unit based on a PEM fuel cell for on-board applications. Journal of fuel cell science and Tech. 3 (2006). 445-451.
- [12] J. Kupecki. Off-design analysis of a micro-CHP unit with solid oxide fuel cells fed by DME. Int. J of Hydrogen Energy 40 (2015) 12009-12022
- [13] S. Pellegrino, A. Lanzini, P. Leone. Techno-economic and policy requirements for the market-entry of the fuel cell micro-CHP system in the residential sector. Applied Energy 143 (2015) 370-382.
- [14] E.J. Naimaster IV, A.K. Sleiti. Potential of SOFC CHP systems for energy-efficient commercial buildings. Energy and Buildings 61 (2013) 153-160.

- [15] L. Barelli, G. Bidini, A. Ottaviano. Part load operation of a SOFC/GT hybrid system: Dynamic analysis. *Applied Energy* 110 (2013) 173–189.
- [16] S. Obara. Power generation efficiency of an SOFC–PEFC combined system with time shift utilization of SOFC exhaust heat. *Int. Journal of Hydrogen Energy*. 35 (2010) 757–767.
- [17] I. Serban, C. Marinescu. Battery energy storage system for frequency support in microgrids and with enhanced control features for uninterruptible supply of local loads. *Int. J of Electrical Power & Energy Systems* 54 (2014) 432–441.
- [18] X. Luo, J. Wang, M. Dooner, J. Clarke. Overview of current development in electrical energy storage technologies and the application potential in power system operation. *Applied energy* 137 (2015) 511–536.
- [19] J.L. Sudworth. The sodium/nickel chloride (ZEBRA) battery. *J Power Sources* 100 (2001) 149–63.
- [20] Cord-H. Dustmann. Advances in ZEBRA batteries. *Journal of Power Sources* 127 (2004) 85–92.
- [21] R. Benato, N. Cosciani, G. Crugnola, S. Dambone Sessa, G. Lodi, C. Parmeggiani, M. Todeschini. Sodium nickel chloride battery technology for large-scale stationary storage in the high voltage network. *Journal of Power Sources* 293 (2015) 127–136.
- [22] <http://www.fiamm.com/en/emea/energy-storage/tecnologie/sodium-nickel.aspx>
- [23] P. Aguiar, D.J.L. Brett, N.P. Brandon. Feasibility study and techno-economic analysis of an SOFC/battery hybrid system for vehicle applications. *Journal of Power Sources* 171 (2007) 186–197.
- [24] M. Bianchi, A. De Pascale, F. Melino. Performance Analysis of an Integrated CHP System with Thermal and Electric Energy Storage for Residential Application. *Applied Energy* 112 (2013) 928–938.
- [25] C. Boigues-Mugnoz, G. Santori, S. McPhail, F. Polonara. Thermochemical model and experimental validation of a tubular SOFC cell comprised in a 1 kW_{el} stack designed for μ CHP applications. *Int. J of Hydrogen Energy* 39 (2014) 21714–21723
- [26] G. Brunaccini, G. Dispenza, M. Ferraro, V. Antonucci, S. Modena. An electrochemical study of a solid oxide fuel cell stack operating at intermediate temperature for distributed generation applications. *Green* 1 (2011) 233–40.
- [27] E. S. Barbieri, P. R. Spina, M. Venturini. Analysis of innovative micro-CHP systems to meet household energy demands. *Applied Energy* 97 (2012) 723–733.
- [28] M. Dentice d’Accadia, M. Sasso, S. Sibilio, L. Vanoli. Micro-combined heat and power in residential and light commercial applications. *Applied Thermal Engineering* 23 (2003) 1247–1259.
- [29] L. Giaccone, A. Canova. Economical comparison of CHP systems for industrial user with large steam demand. *Applied Energy* 86 (2009) 904–914.
- [30] <http://www.htceramix.ch/upload/HoTbox.pdf>
- [31] E. Barbieri, A. De Pascale, C. Ferrari, F. Melino, M. Morini, A. Peretto, M. Pinelli, Performance evaluation of the integration between a Thermo-Photo-Voltaic generator and an Organic Rankine Cycle, *Transaction of the ASME, Journal of Engineering for Gas Turbines and Power*, Vol. 134, pag. 102301-1/10, October 2012
- [32] M. Bianchi, A. De Pascale, P. R. Spina. Guidelines for Residential Micro-CHP Systems Design, *Applied Energy*, Volume 97 (2012) 673–685.
- [33] Directive 2004/08/EC of the European Parliament and of the Council, *Official Journal of the European Union* 21.2.2004, pp. 50–60.

Figure Captions

Figure 1: SOFC internal layout.

Figure 2: SOFC experimental performance: a) V, I and Power during start-up and base load operation b) base load stack temperature values in different cells.

Figure 3: SOFC experimental performance: a) base-load temperature at cathode inlet and afterburner outlet ; b) part load profile of exhaust gas temperature and mass flow.

Figure 4: SOFC experimental performance: a) polarization and power curves; b) part-load el./th. efficiency vs load.

Figure 5: a) SNC battery power vs SOC; b) SNC battery charging V-I characteristics.

Fig. 6. Layout of the energy system network with components and power flows. “Thermal stand-by” and “electric stand-by” power flows are shown in red and blue dotted lines, fuel power flows are in green.

Figure 7: Calculation routines developed considering (a) the electric stand-by configuration and (b) the thermal stand-by configuration.

Figure 8: Thermal flows subroutine.

Figure 9: Electric flows subroutine.

Figure 10: The hot gas line for CHP operation with “thermal stand-by”.

Figure 11: Electric and thermal USER hourly mean power demand, normalized with max value: a) yearly monotonic curves; b) typical daily profiles.

Figure 12: Comparison between thermal and electric stand-by for the different micro-CHP systems: a) prime mover operating hours; b) SNC battery stand-by hours.

Fig. 13. Comparison between thermal and electric stand-by for the different micro-CHP systems: a) Thermal system efficiency; b) Electric system efficiency.

Figure 14: Primary energy savings per unit of installed power - Comparison of SOFC and other micro-CHP systems: a) electric-stand-by; b) thermal stand-by.

Figure 15: Admissible investment cost - Comparison of SOFC and other micro-CHP systems: a) electric-stand-by; b) thermal stand-by.

Table Captions

Table 1: SOFC nameplate data.

Table 2: SOFC steady-state data reached during the tests.

Table 3: SNC battery main characteristics

Table 4: SOFC – SNC energy balance for one thermal-year of operation - domestic user.

Table 5: Conventional and innovative μ -CHP systems considered for comparison purpose.

Table 6: Values assumed for economic analysis.

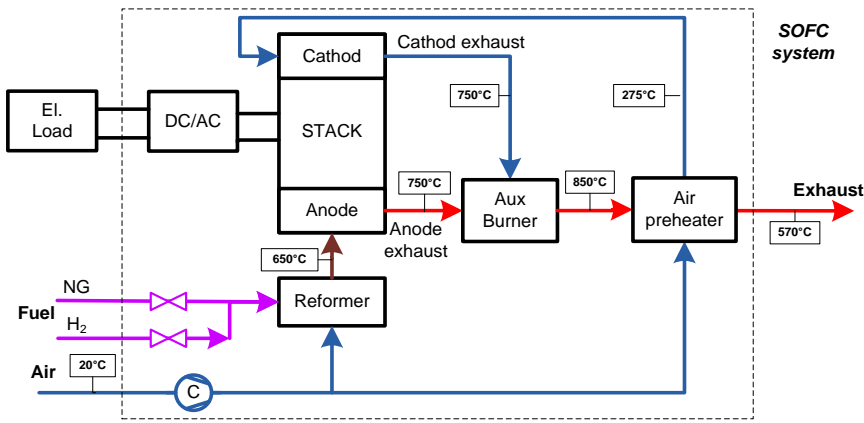


Fig. 1. SOFC internal layout.

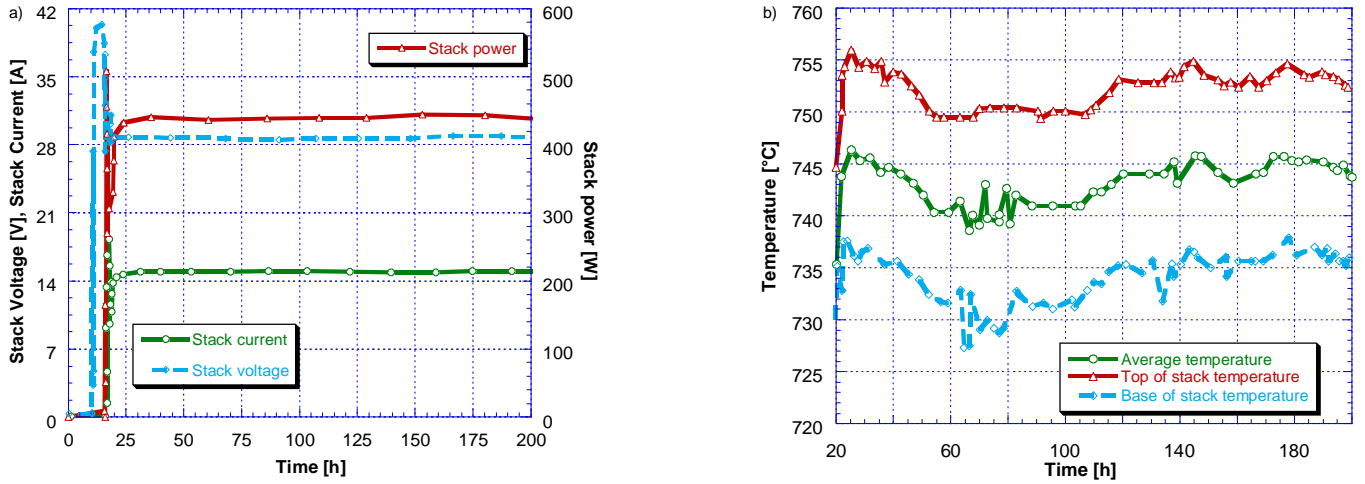


Fig. 2. SOFC experimental performance: a) V, I and Power during start-up and base load operation b) base load stack temperature values in different cells.

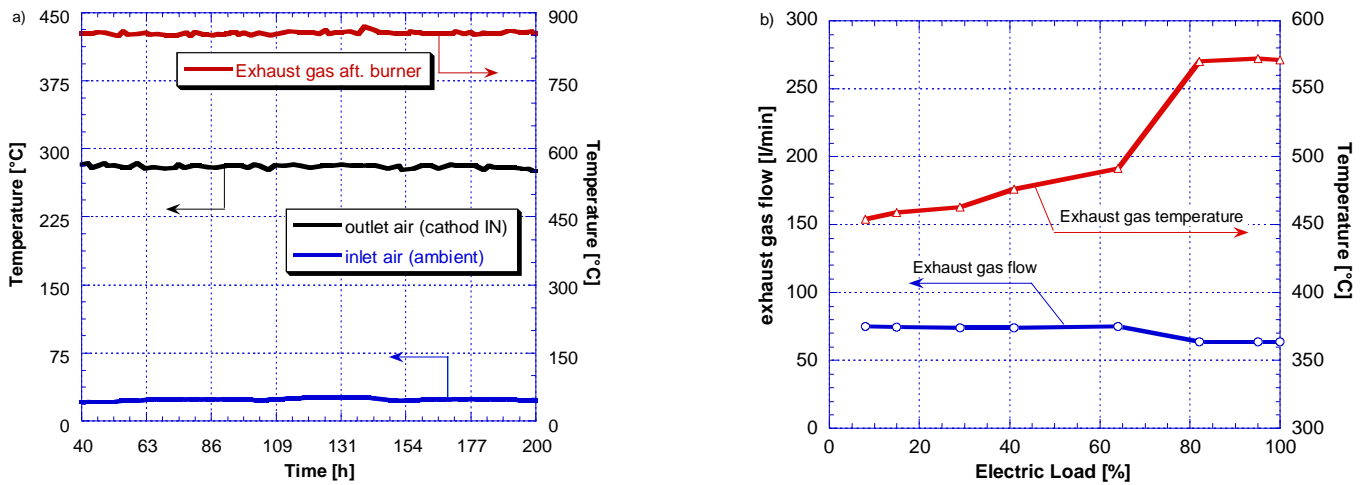


Fig. 3. SOFC experimental performance: a) base-load temperature at cathode inlet and afterburner outlet; b) part load profile of exhaust gas temperature and mass flow.

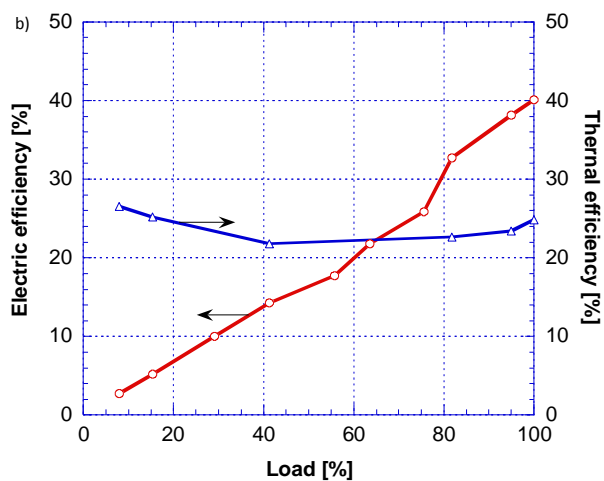
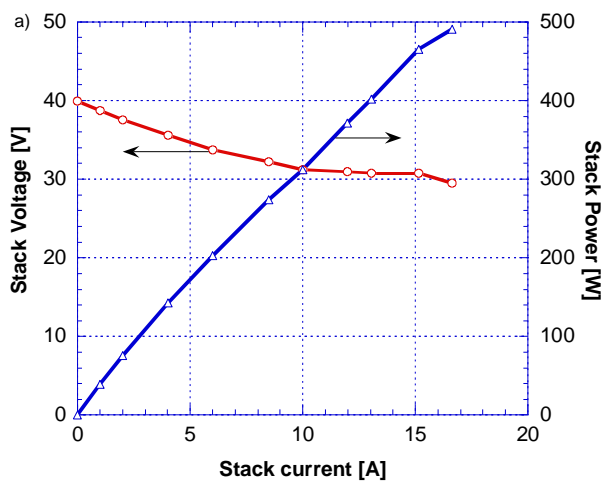


Fig. 4. SOFC experimental performance: a) polarization and power curves; b) part-load el./th. efficiency vs load.

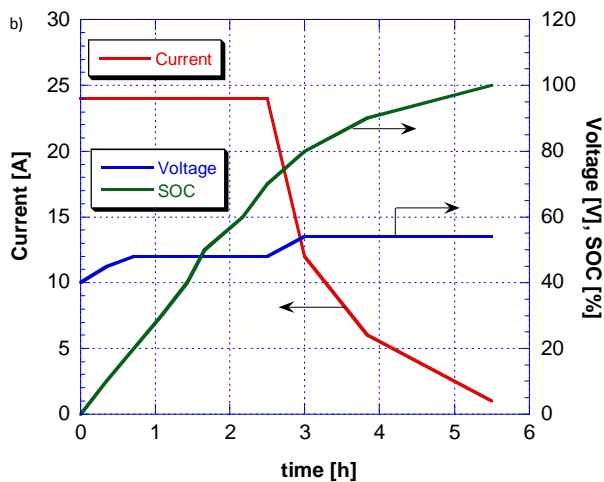
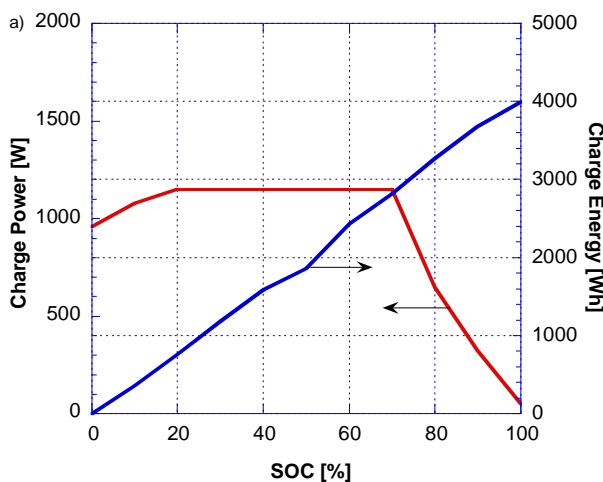


Fig. 5. a) SNC battery power vs SOC; b) SNC battery charging V-I characteristics.

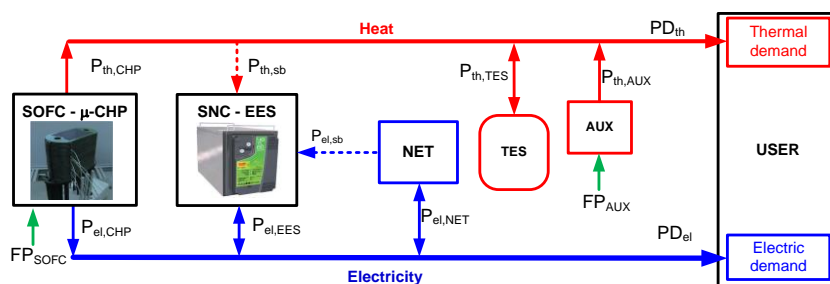


Fig. 6. Layout of the energy system network with components and power flows. "Thermal stand-by" and "electric stand-by" power flows are shown in red and blue dotted lines, fuel power flows are in green.

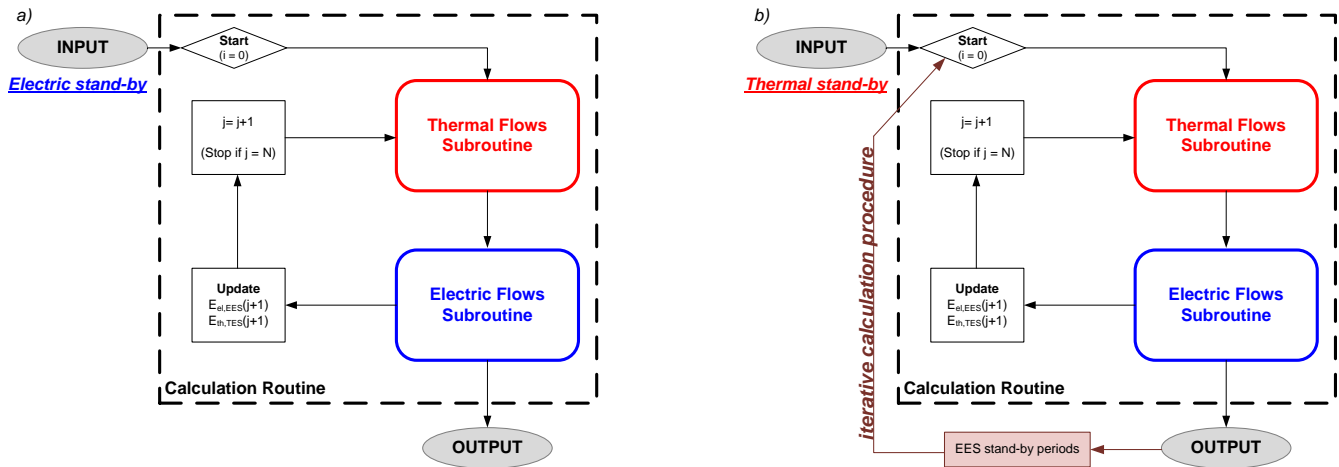


Fig. 7. Calculation routines developed considering (a) the electric stand-by configuration and (b) the thermal stand-by configuration.

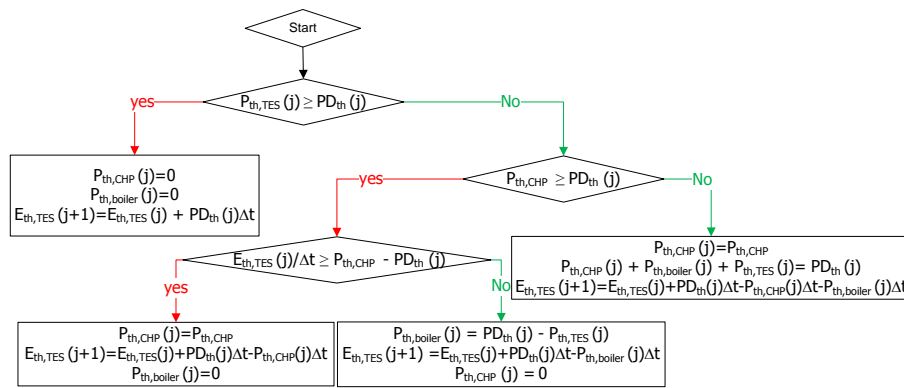


Fig. 8. Thermal flows subroutine.

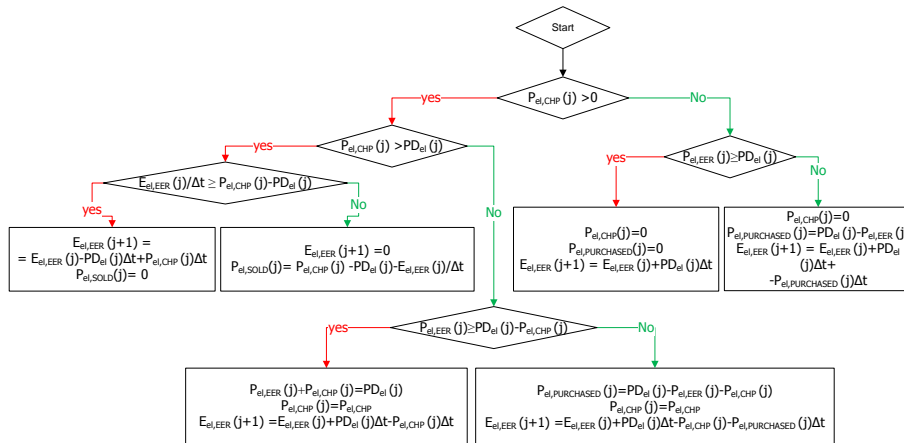


Fig. 9. Electric flows subroutine.

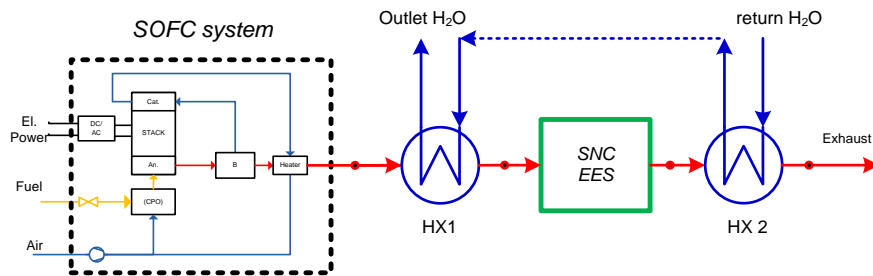


Fig. 10. The hot gas line for CHP operation with "thermal stand-by".

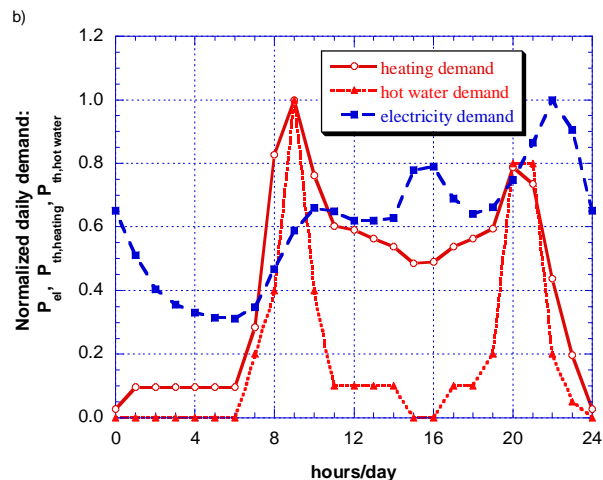
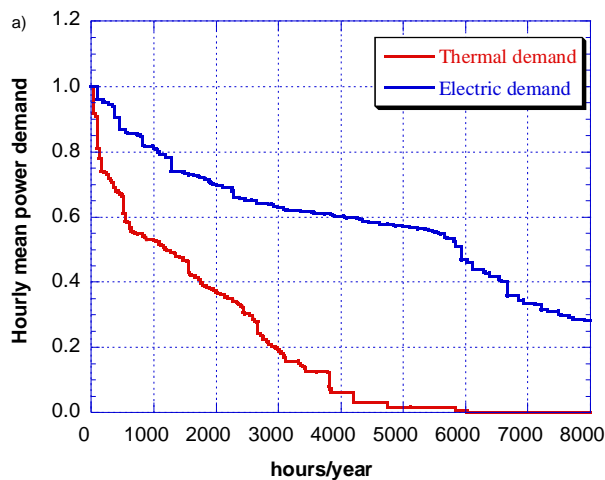


Fig. 11. Electric and thermal USER hourly mean power demand, normalized with max value: a) yearly monotonic curves; b) typical daily profiles.

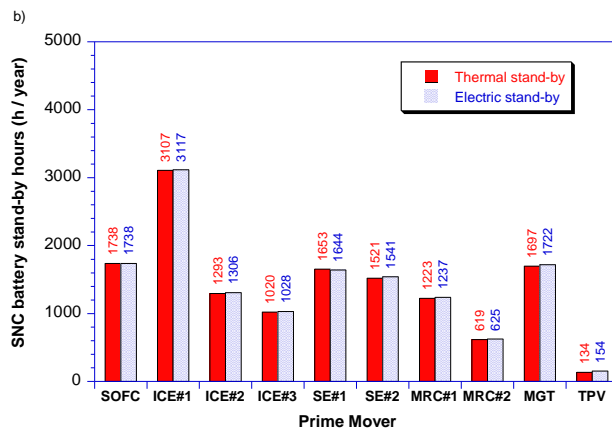
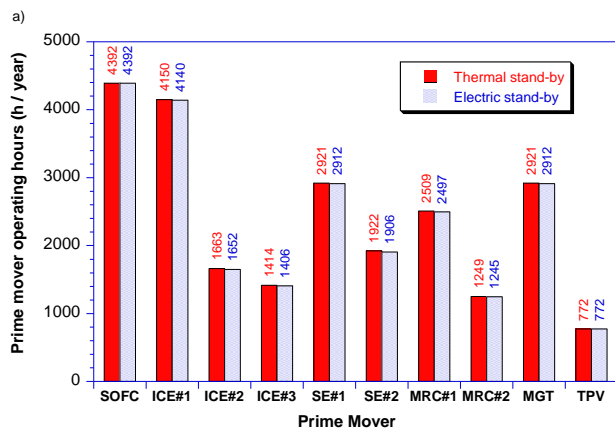


Fig. 12. Comparison between thermal and electric stand-by for the different micro-CHP systems: a) prime mover operating hours; b) SNC battery stand-by hours.

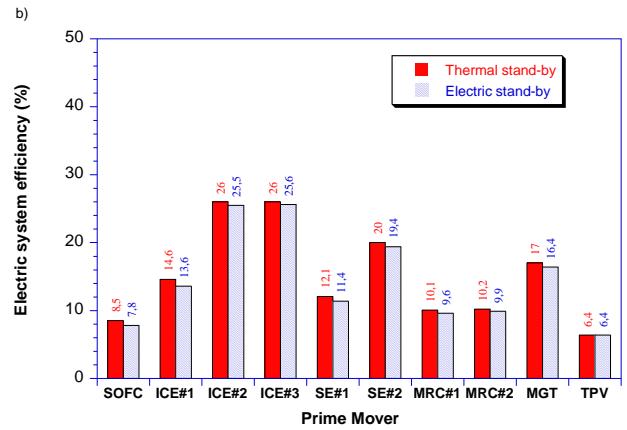
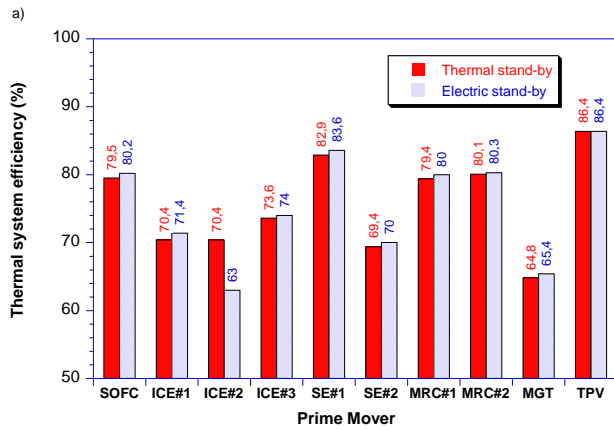


Fig. 13. Comparison between thermal and electric stand-by for the different micro-CHP systems: a) Thermal system efficiency; b) Electric system efficiency.

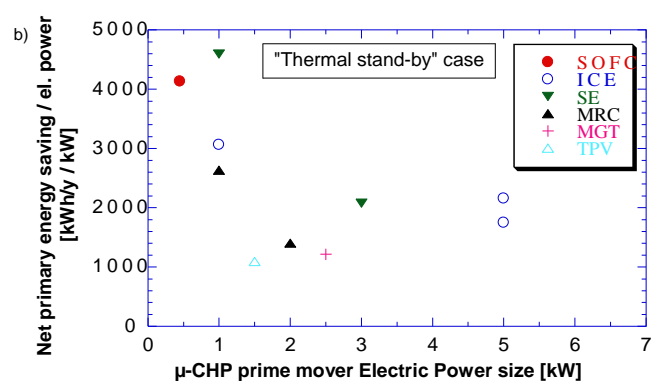
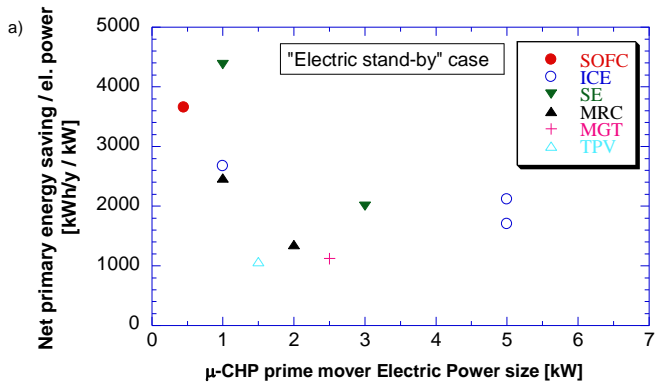


Fig. 14. Primary energy savings per unit of installed power - Comparison of SOFC and other micro-CHP systems: a) electric-stand-by; b) thermal stand-by.

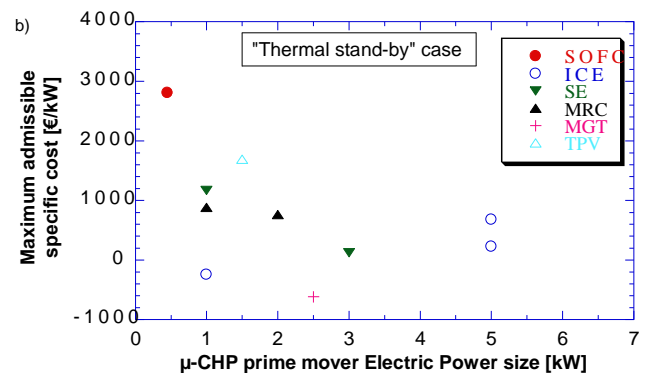
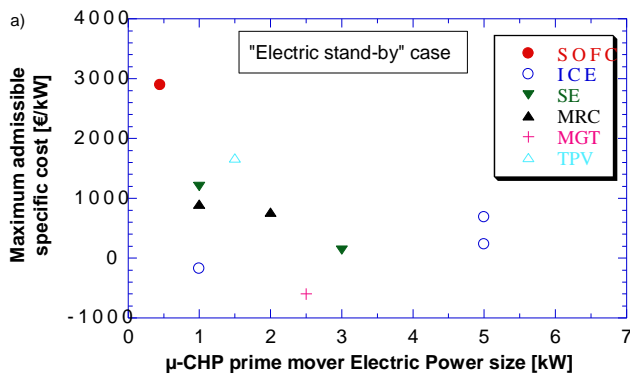


Fig. 15. Admissible investment cost - Comparison of SOFC and other micro-CHP systems: a) electric-stand-by; b) thermal stand-by.

580
581

582
583
584

585
586
587

588
589
590
591

Table 1. SOFC nameplate data.

<i>Parameter</i>	<i>Unit</i>	<i>value</i>
Electric power output	kW	05-0.6
Max power density	W/cm ²	0.375
Nominal electric DC efficiency	-	45%
Peak DC electric efficiency	-	50 %
Operating temperature	°C	750
weight	kg	17.5

Table 2. SOFC steady-state data reached during the tests.

<i>Parameter</i>	<i>unit</i>	<i>value</i>
Electric power output	W	490
Stack voltage	V	29.0
Stack current	A	16.6
Natural gas flow	slpm	2.0
Air flow	slpm	114
Exhaust	slpm	64.0
Heating up time	min	220

Table 3. SNC battery main characteristics.

<i>Parameter</i>	<i>unit</i>	<i>value</i>
Capacity	Ah	80
Energy	kWh	4
Voltage	V	48
Maximum voltage	V	56
Minimum voltage	V	40
Current	A	50
Peak power	kW	10
Cells number	-	50

592

Table 4. SOFC – SNC energy balance for one thermal-year of operation - domestic user

593

594

595

596

597

598

599

600

601

602

603

604

605

606

607

608

609

610

611

612

613

614

615

616

617

618

THERMAL ENERGY yearly balance			ELECTRIC ENERGY yearly balance		
Energy term [kWh], (share of USER demand)	<i>Electric stand-by scenario</i>	<i>Thermal stand-by scenario</i>	Energy term [kWh], (share of USER demand)	<i>Electric stand-by scenario</i>	<i>Thermal stand-by scenario</i>
USER demand	20000	20000	USER demand	1458	1458
SOFC output	2393 (12%)	2393 (12%)	SOFC output	2152 (147%)	2152 (147%)
From SOFC to USER	1693 (8.5%)	1534 (7.7%)	From SOFC to NET	499 (34%)	691 (47%)
EES thermal absorption	0 (0%)	191 (1.0%)	EES electric absorption	191 (13%)	0 (0%)
Stored and delivered by TES	700 (3.5%)	667 (3.3%)	Stored in EES	556 (38%)	556 (38%)
From AUX	17607 (88%)	17798 (89%)	From NET	0 (0%)	0 (0%)

619

Table 5. Conventional and innovative μ -CHP systems considered for comparison purpose.

620

621

622

623

624

625

626

627

628

629

630

631

632

633

634

635

636

637

638

639

640

641

642

643

644

645

646

647

648

649

650

651

652

653

654

655

Considered μ -CHP systems in the range of power size up to 5 kW										
	SOFC	ICE #1	ICE #2	ICE #3	SE #1	SE #2	MRC#1	MRC#2	MGT	TPV
P_{el} [kW]	0.5	1.0	5.0	5.0	1.0	3.0	1.0	2.0	2.5	1.5
η_{el} [%]	40	20	26	26	13	20	10	10	17	5
η_{th} [%]	37	65	63	74	80	70	80	84	64	86.5
C=P_{el}/Q_{th}	1.08	0.31	0.41	0.35	0.16	0.29	0.13	0.12	0.26	0.058
TES [m³]	0.5	0.5	1.0	1.0	0.5	0.5	0.5	0.5	0.5	1.0

619

620

621

622

623

624

625

626

627

628

629

630

631

632

633

634

635

636

637

638

639

640

641

642

643

644

645

646

647

648

649

650

651

652

653

654

655

656

657

658

659

660

661

662

663

664

665

666

667

668

669

670

671

672

673

674

675

676

677

678

679

680

681

682

683

684

685

686

687

688

689

690

691

692

693

694

695

696

697

698

699

700

701

702

703

704

705

706

707

708

709

710

711

712

713

714

715

716

717

718

719

720

721

722

723

724

725

726

727

728

729

730

731

732

733

734

735

736

737

738

739

740

741

742

743

744

745

746

747

748

749

750

751

752

753

754

755

756

757

758

759

760

761

762

763

764

765

766

767

768

769

770

771

772

773

774

775

776

777

778

779

780

781

782

783

784

785

786

787

788

789

790

791

792

793

794

795

796

797

798

799

800

801

802

803

804

805

806

807

808

809

810

811

812

813

814

815

816

817

818

819

820

821

822

823

824

825

826

827

828

829

830

831

832

833

834

835

836

837

838

839

840

841

842

843

844

845

846

847

848

849

850

851

852

853

854

855

856

857

858

859

860